Materials Research Proceedings **24** (2022) 240-246 https://doi.org/10.21741/9781644902059-35

Microstructure and Mechanical Properties of Dissimilar Friction Welded B500B-1.4021 Steel Joint

OSTROMĘCKA Małgorzata

Instytut Kolejnictwa (The Railway Research Institute), Materials & Structure Laboratory, 50 Chłopicki Street, 04-275 Warsaw, Poland

mostromecka@ikolej.pl

Keywords: Rotary Friction Welding, Dissimilar Joint, Hardness, Tensile Test, Microstructure, Martensitic Stainless Steel, Reinforcing Steel

Abstract. In this study, unalloyed reinforcing steel (B500B) is merged with martensitic stainless steel (1.4021). The paper presents microstructural observation, hardness measurements, and tensile test results of this dissimilar joint as-welded. In this specific case, no heat treatment is demanded. The joint is a part of the pile foundation for railway traction lines.

Introduction

Joining dissimilar materials offers the potential to utilize the advantages of different materials and provide unique solutions to engineering requirements. The main reason for dissimilar joining is to combine good mechanical properties of one material and, for example, good corrosion resistance of the second material. But very often, the most important is an economic reason [1,2].

Friction welding is well established as highly productive and one of the most economical methods in joining similar and dissimilar metals. The process is readily used by producers, especially since it enables joint creation in circumstances that exclude other welding methods.

One complex combination of the dissimilar joint is between unalloyed and high alloyed martensitic steel [2]. Such a combination is not mentioned in PN-EN ISO 15620: 2019 [3] as weldable with a friction welding method. Not many publications concerning such a joint, but this is an application in railway infrastructure. The reinforcing steel, which offers good weldability, is merged with martensitic stainless steel that is not easily welded, often needs to be preheated, and uses special welding consumables. This joint is used in concrete piles that act as foundations and anchors for traction lines. The pile is manufactured of reinforced concrete where reinforcing is made of B500B ribbed steel and anchor of 1.4021 martensitic stainless steel. The joints are covered with the concrete and are not subject to shear stresses until the concrete cover is still. The alternate solution for this application is to combine reinforcing steel and stainless austenitic steel, but this kind of joint is well described in the literature. Therefore, this is not a subject of the paper. The only quality control of these joints is conducted according to Factory Production Control. The final pile's quality guidelines do not provide for testing these joints, even at the stage of authorization for placing in service.

Fig. 1. The joint after welding

Materials Research Proceedings **24** (2022) 240-246 https://doi.org/10.21741/9781644902059-35

Research Methodology

Materials and Welding Parameters. The manufacturer company prepared the joints (Fig.1) according to approved welding technology using the ZT3-22 machine. Each joint was made between a ribbed reinforcing steel bar and martensitic steel 1.4021/X20Cr13 (AISI 420) anchor. The chemical composition of base materials and technological conditions are presented in Tables 1, 2, and 3. The microstructure of the base materials is shown in Fig.2.

Table 1. *Chemical composition (% by mass) for B500B steel according to PN-EN 10080:2007 [4], the base material 1*

B500B steel	C [%]	N [%]	S [%]	P [%]	Cu [%]	Carbon equivalent C_{eq}
Cast analysis	≤ 0,22	≤ 0,012	≤ 0,050	≤ 0,050	≤ 0,80	≤ 0,50
Product analysis	≤ 0,24	≤ 0,013	≤ 0,055	≤ 0,055	≤ 0,85	≤ 0,52

Table 2. *Chemical composition (% by mass) for martensitic stainless steel 1.4021/X20Cr13 according to PN-EN 10088-3: 2015 [5], the base material 2.*

C [%]	Mn [%]	Si [%]	P [%]	S [%]	Cr [%]	Ni [%]	Cu [%]
0.16 - 0.25	<1.5	<1.0	<0.04	<0.03	12.0 - 14.0	-	-

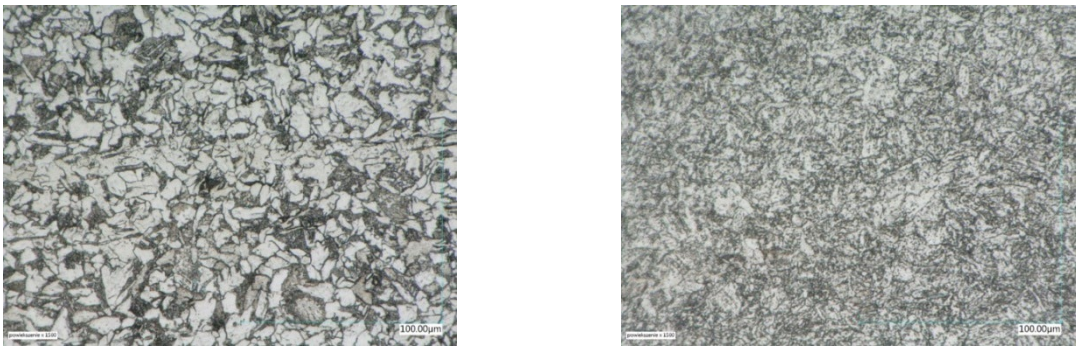

Fig. 2. *Microstructure of base materials: reinforcing steel on the left and martensitic stainless steel on the right (description in the text).*

Table 3. *Welding parameters.*

Rotational speed V [rpm]	Friction pressure F_t [kG/cm^2]	Forging pressure F_s [kG/cm^2]	Friction time t_t [s]	Forging time t_s [s]	Welded area [mm^2]
800	115	140	5	6	490

Materials Research Proceedings **24** (2022) 240-246 https://doi.org/10.21741/9781644902059-35

Microstructural observation, hardness, and tensile test. The metallographic investigations were carried out on polished and etched surfaces. Etching was executed using 4% Nital solution on the B500B steel side and then with Adler's reagent to reveal the martensitic microstructure and plastic deformation lines. Keyence VHX-900F microscope was used to characterize microstructure.

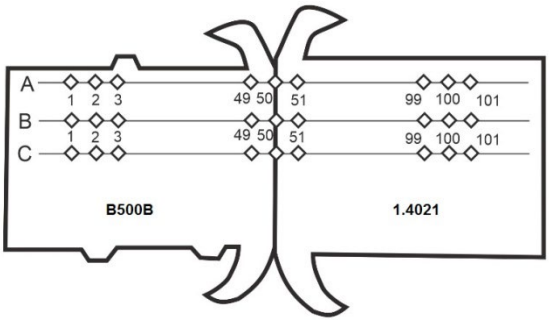

Fig. 3. *Microhardness measurement scheme*

HV0.1 Vicker's microhardness measurements were executed on polished surfaces across the weld. KB Prüftechnik GmbH automatic hardness tester type KB50BYZ-FA was used according to PN-EN ISO 6507-1: 2018-05 [6] standard. Three lines were made on each of the samples, measuring 101 points at a distance of 0.2 mm, while the measuring lines were spaced 5 mm apart. The measuring scheme is presented in Fig.3.

Instron Schenk Testing System LFV 4000-2500 was used on two types of samples: on round tensile specimens where the weld center was marked with red lacquer and on specimens without any special preparation just as they work.

Results and Discussion.

Microstructure and hardness. The microstructure of base material 1 - B500B steel comprises outer tempered martensite, an inner core of ferrite-pearlite (Fig. 2 on the left), and between a narrow bainitic transition zone. The maximum hardness is achieved near the ribs side (Fig. 9 left side of the A line), decreasing towards the center. The macrostructure presented in Fig.4 reveals a darker area of peripheries by the rebar side. In the core of the bar close to the weld line, grain refinement can be observed, and the grain size increases toward the distance of the weld line (Fig.5). Closer to the ribs side, grains growth appears instead of refinement, and near the weld, several secondary surfaces are part of a partially mixed region (Fig.6). The thermo-mechanically affected zone of the reinforcing steel side was presented in Fig.8.

The microstructure of base material 2 – stainless steel consists of tempered martensite with carbide precipitations (Fig. 2 – right side). The weld line is very narrow, but the thermo-mechanically affected zone (TMAZ) is about 400 μm near the center and broader on the peripheries (Fig. 4). Next to the flash, many partially mixed regions can be observed. In the core, there are many deformation lines and bands (the darker areas in Fig.7).

Fig. 4. *Macrostructure of the joint with asymmetrical flashes*

Fig. 5. *Microstructure of reinforcing steel in the axis of the specimen. The white region is an unetched martensite steel side.*

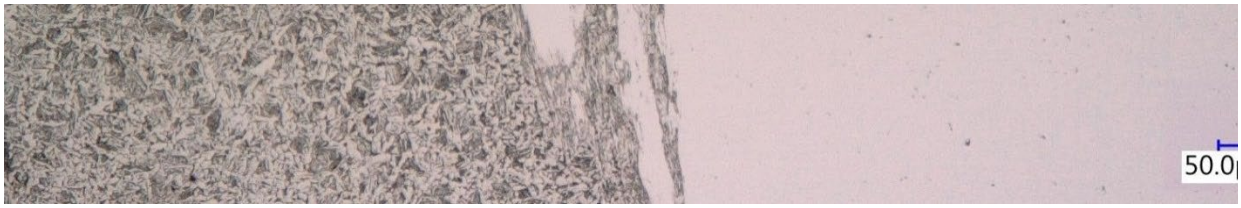

Fig. 6. *Microstructure of reinforcing steel in the area closer to the edge of the specimen.*

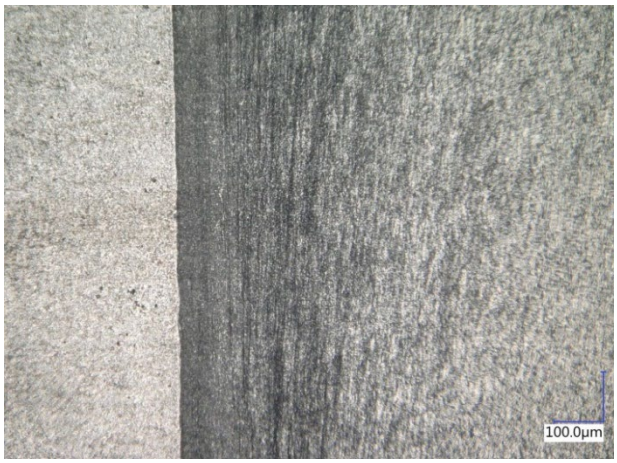

Fig. 7. *Thermo-mechanically affected zone (TMAZ) in the 1.4021 steel (on the right from weld)*

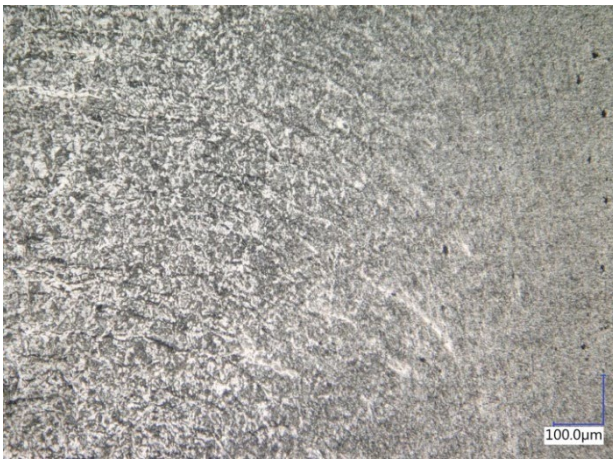

Fig. 8. *Thermo-mechanically affected zone (TMAZ) on B500B reinforcing steel side.*

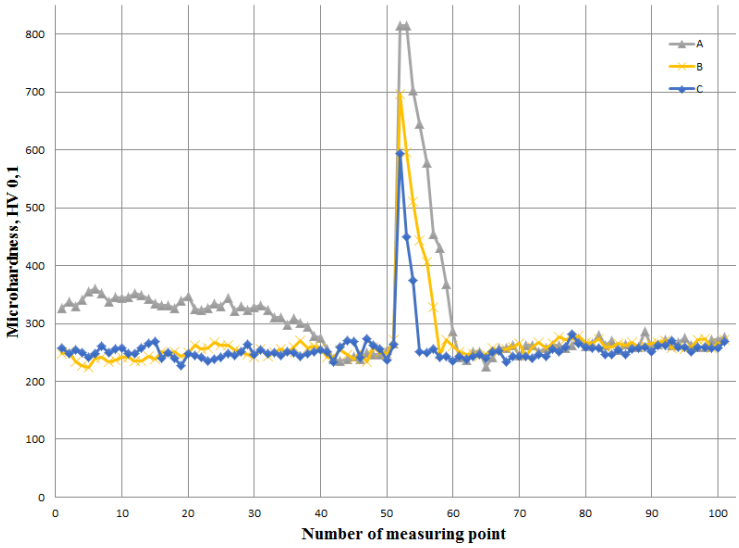

Fig. 9. *Microhardness profiles*

Materials Research Proceedings **24** (2022) 240-246 https://doi.org/10.21741/9781644902059-35

The hardness of the base materials cores exhibits similar values of about 260 HV_{01}. The hardness increases rapidly near the weld line by the martensitic steel side. Line A presents measurement near the specimen's outer side, and the highest value is 814 HV_{01}. In line C, the highest measurement is 594 $HV_{01,}$ and in line B – 696 HV_{01}. In the TMAZ of reinforcing steel, the hardness slightly increases, but close to the outer area, it decreases to the base material value. The difference in microhardness value between the center and outer region can be attributed to the supplied heat distribution, and therefore differences in microstructure arise [7]. The hardness increase in the area close to the weld is a common situation, and it can be explained by quenched martensite microstructure formation [1, 8]. In special quality applications such as the automotive industry, such a joint would need a post-weld treatment to lower the hardness in the weld. Another possibility is to use a transition layer [2, 9]. The hardness is the end value in the investigated joint, and technology does not demand a post-weld treatment or flash removal.

Tensile test. The chosen tensile test specimens after fracture are presented in Fig.10. The welded joints represent a brittle fracture with no necking and plastic deformation. The microstructure observation and hardness measurements let us expect that the presented specimens are broken close to the weld in the thermo-mechanically affected zone of the stainless steel 1.4021.

a b

Fig. 10. *The view of fractured sample numbers 2 (a) and 8 (b) (Table 4,5)*

Table 4. *Tensile test samples as-welded with flashes*

Sample number	Tested area of weld cross-section [mm^2]	Tensile force F_m [kN]	Tensile strength R_m,[MPa]	Fractured in
1	490	332.50	678	base material BM1
2		327.28	668	weld
3		333.19	680	base material BM1
4		328.15	670	base material BM1
5		328.26	670	base material BM1

Table 5 *Round polished tensile test samples without flashes*

Sample number	Tested area of weld cross-section [mm^2]	Tensile force F_m [kN]	Tensile strength R_m,[MPa]	Fractured in
6	380	240.82	630	weld
7		253.10	666	weld
8		245.70	647	weld

Conclusions

The rotary friction welding process successfully carried out dissimilar material joining B500B reinforcing to 1.4021 martensitic steel, and the microstructure and mechanical properties were studied. The summary of the observations is as follows:

– the affected zone near the weld joint is not homogenous and presents several areas with different microstructure morphologies and mechanical properties.
– the hardness measurements performed on the joint present the highest hardness at the thermo-mechanically deformed zone of the stainless steel. It causes a reduction in ductility of the weld joint.
– the observations confirm that, in this case, flash removal is not recommended.

References

[1] M.R. Abbasai, Kh. Gheisari. Microstructure and Mechanical Properties of the Friction Welded Joint between X53CrMnNiN219 and X45CrSi93 Stainless Steel, Journal of Advanced Materials and Processing 5 (2017) 81-92.

[2] A. Ambroziak. Zgrzewanie tarciowe materiałów o różnych właściwościach. Oficyna Wydawnicza Politechniki Wrocławskiej, Wrocław, 2011.

[3] PN-EN ISO 15620:2019-07 Friction welding of metallic materials.

[4] PN-EN 10080:2007 Stal do zbrojenia betonu – Spajalna stal zbrojeniowa – Postanowienia ogólne.

[5] PN-EN 10088-3: 2015-01 Stale odporne na korozję – Część 3: Warunki techniczne dostawy półwyrobów, prętów, walcówki, drutu, kształtowników i wyrobów o powierzchni jasnej ze stali nierdzewnych ogólnego przeznaczenia.

[6] PN-EN ISO 6507-1: 2018-05 Metale – Pomiar twardości sposobem Vickersa – Część 1: Metoda badania.

[7] B.S Taysom, C.D. Sorensen. Controlling Martensite and Perlite Formation with Cooling Rate and Temperature Control in Rotary Friction Welding. International Journal of Machine Tools & Manufacture, 150 (2020) art. 103512. https://doi.org/10.1016/j.ijmachtools.2019.103512

[8] M. Demouche, E.H. Ouakdi, R. Louahdi. Effect of Welding Parameters on the Microstructure and Mechanical Properties of Friction-Welded Joints of 100Cr6 Steel. Iranian Journal of Materials Science and Engineering 16 (2019) 24-31. https://doi.org/10.22068/ijmse.16.2.24

[9] N. Sridharan, E. Cakmak, B. Jordan. Design, Fabrication, and Characterization of Graded Transition Joints. Welding Journal 96 (2017) 295-306.

[10] C.S. Paglia, R.G. Buchheit. Microstructure, microchemistry and environmental cracking susceptibility of friction stir welded 2219-T87. Materials Science and Engineering A 429 (2009) 107-114. https://doi.org/10.1016/j.msea.2006.05.036